

# Characteristics of oriented $\text{LaNiO}_3$ thin films fabricated by the sol–gel method

Shinichi Miyake, Shinobu Fujihara \*, Toshio Kimura

Department of Applied Chemistry, Faculty of Science and Technology, Keio University, 3-14-1, Hiyoshi, Kohoku-ku, Yokohama 223-8522, Japan

Received 4 September 2000; received in revised form 2 November 2000; accepted 30 November 2000

## Abstract

We fabricated  $\text{LaNiO}_3$  (LNO) thin films on  $\text{SiO}_2$  glass, (100)  $\text{SrTiO}_3$  (STO), (100) Si and  $\text{CeO}_2$ -covered (100) Si substrates by the sol–gel method. The deposited films were heat-treated at 700°C with various conditions, duration and atmosphere. Preferentially (100)-oriented, polycrystalline LNO films were obtained on STO and Si. It was also found that orientated films could be formed even on  $\text{SiO}_2$  glass and  $\text{CeO}_2$ -covered (100) Si substrates by altering the heating process. We investigated a relationship between the resistance and the crystallite size of the LNO films. The sheet resistance of LNO decreased with increasing crystallite size of LNO. The resistivity and sheet resistance of LNO/STO at 300 K were 340  $\mu\Omega\cdot\text{cm}$  and 33.8  $\Omega/\square$ , respectively, and those values of LNO/ $\text{CeO}_2$ /Si at 300 K were 460  $\mu\Omega\cdot\text{cm}$  and 28.8  $\Omega/\square$ . © 2001 Elsevier Science Ltd. All rights reserved.

**Keywords:**  $\text{CeO}_2$ ; Electrical conductivity; Films; Perovskites; Sol–gel processes

## 1. Introduction

Perovskite ferroelectric thin films have been attracting much attention for applications to a ferroelectric random access memory (FeRAM). Although a metal film like Pt or Ir is often used as an electrode, it has weak adhesion to a Si wafer and tends to cause ferroelectric fatigue due to oxygen deficiency.<sup>1</sup> Oxides, especially perovskite-type oxides, with metallic conductivity have been studied as an alternative electrode.  $\text{LaNiO}_3$  (LNO) has the pseudo-cubic perovskite structure ( $a=3.84 \text{ \AA}$ ), low resistivity (225  $\mu\Omega\cdot\text{cm}$ ) and good metallic conductivity.<sup>2,3</sup> (100)-oriented LNO films can be utilized to control orientation of the perovskite-type ferroelectric thin film deposited successively. Therefore, highly (100)-oriented LNO is a promising candidate for the electrode as well as the substrate for the ferroelectric thin films.<sup>4–10</sup> In this work we investigated first the effects of sol–gel processing parameters on the orientation and the electrical properties of LNO thin films. Then  $\text{LaNiO}_3/\text{CeO}_2/\text{Si}$  structure was prepared as an MIS (Metal-Insulator-Semiconductor) structure.

## 2. Experimental procedure

$\text{La}(\text{NO}_3)_3 \cdot 6\text{H}_2\text{O}$  (0.002 mol) was dissolved in 2-methoxyethanol (9 ml) and monoethanolamine (MEA) (1 ml), and then  $\text{Ni}(\text{CH}_3\text{COO})_2 \cdot 4\text{H}_2\text{O}$  (0.002 mol) was added to the solution. The resultant solution was deposited on  $\text{SiO}_2$  glass, (100)  $\text{SrTiO}_3$  (STO), (100) Si and  $\text{CeO}_2$ -coated (100) Si substrates by the spin-coating technique at 2700 rpm for 30 s. After deposition, the deposited substrates were heated at 700°C for 1–20 min in air. Two kinds of heating processes were adopted. In one process, the deposited substrate was put on a plate at room temperature and then heated so that the films could be heated uniformly in the furnace (process 1). In the other process, the deposited substrate was put on a pre-heated plate at 700°C so that the film should be heated first from the bottom of the substrate (process 2). After repeating the deposition 5 times, the sample was finally annealed at 700°C in a flowing oxygen atmosphere. To form the  $\text{CeO}_2$  insulator layer,  $\text{Ce}(\text{NO}_3)_3 \cdot 6\text{H}_2\text{O}$  (0.0015 mol) was dissolved in acetylacetone (10 ml). The solution was refluxed at 100°C for 1 h in the presence of zeolite to remove  $\text{H}_2\text{O}$ .  $\text{CeO}_2$  thin films were deposited on (100) Si by the spin-coating technique. The deposited substrate was heated at various temperatures between 400 and 700°C for 1 min by rapid heating in

\* Corresponding author. Tel.: +81-45-566-1581; fax: +81-45-566-1551.

E-mail address: shinobu@apple.keio.ac.jp (S. Fujihara).

air, this procedure was repeated 5 times, and finally the sample was annealed for 1 h at the same temperature in air. The phases were identified by an X-ray diffraction (XRD)  $\theta$ - $2\theta$  scan using  $\text{CuK}\alpha$  radiation. The crystallite size of LNO was calculated by Scherrer formula from XRD profiles of the films. Surface and thickness of the films were observed by field emission scanning electron microscopy (FESEM). The resistivity of the sheet was measured by the four-points method where the sheet resistance ( $\rho_s$ ) is defined by volume resistivity  $\rho$  and thickness of the sample  $t$  as  $\rho_s = \rho/t$  and unit is expressed by  $\Omega/\square$ . The electrical resistivity ( $\rho$ ) of LNO was measured by the four probe method.

### 3. Results

Fig. 1 shows the XRD  $\theta$ - $2\theta$  scan profiles of LNO deposited on (a)  $\text{SiO}_2$  glass, (b) STO and (c) Si substrates with heating at  $700^\circ\text{C}$  for 10 min through process 1 and annealing at  $700^\circ\text{C}$  in a flowing oxygen for 1 h. The strong (100) and (200) peaks of LNO (pseudo-cubic) are observed in LNO/STO and LNO/Si. We calculated orientation factor  $F$  as defined by Lotgering.<sup>11</sup> The  $F$  values were (a)  $F=0.07$ , (b)  $F=0.97$  and (c)  $F=0.99$  for LNO/ $\text{SiO}_2$  glass, LNO/STO and LNO/Si, respectively. This result indicates that the growth of LNO is affected by the substrate structure; STO ( $a=3.95\text{ \AA}$ ) and Si ( $a=5.43\text{ \AA}$ ) have an excellent lattice match with LNO ( $a=3.84$  and  $\sqrt{2}a=5.43\text{ \AA}$ ). The resistivity and sheet resistance of LNO/STO at 300 K were  $340\text{ }\mu\Omega\cdot\text{cm}$  and  $33.8\text{ }\Omega/\square$ , respectively, and those of LNO/Si were  $630\text{ }\mu\Omega\cdot\text{cm}$  and  $43.5\text{ }\Omega/\square$ , respectively. These values were lower than those of LNO/ $\text{SiO}_2$ , 1528  $\mu\Omega\cdot\text{cm}$  and  $90.3\text{ }\Omega/\square$ , with relatively small  $F$ .

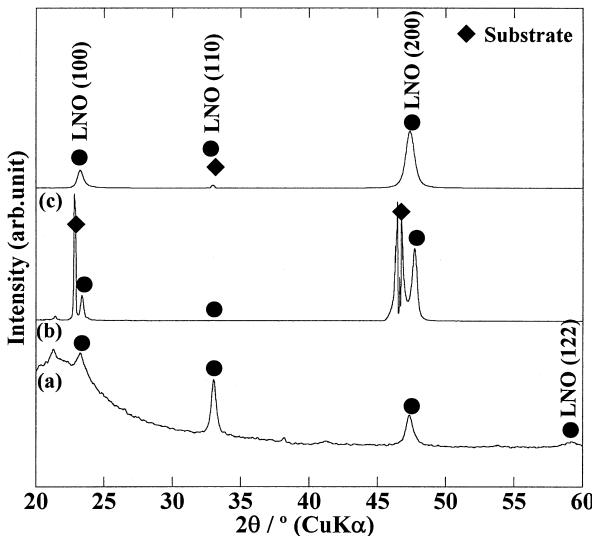


Fig. 1.  $\theta$ - $2\theta$  XRD profiles of  $\text{LaNiO}_3$  thin films on (a)  $\text{SiO}_2$  glass, (b) (100)  $\text{SrTiO}_3$  and (c) (100) Si substrates heated at  $700^\circ\text{C}$  and annealed at  $700^\circ\text{C}$  for 1 h in a flowing oxygen by process 1.

We fabricated LNO thin films on  $\text{SiO}_2$  glass substrates by process 2. Fig. 2 shows the XRD  $\theta$ - $2\theta$  scan profiles of LNO films heated at  $700^\circ\text{C}$  for (a) 1 min, (b) 5 min, (c) 10 min and (d) 20 min and annealed in a flowing oxygen for 5 h. The LNO films made by process 2 have the higher degree of (100)-orientation than those made by process 1. The orientation factor of films was between  $F=0.91$  and 0.95. In spite of almost the same in the  $F$  values, the sheet resistance of the films was different; 53.5, 114, 88.6 and  $128\text{ }\Omega/\square$  for the samples in Fig. 2(a), (b), (c) and (d), respectively. The  $F$  values, the crystallite size and the sheet resistance of  $\text{LNO}/\text{SiO}_2$  films were exhibited in Table 1. This difference is originated from crystallite size of LNO. The relationship between crystallite size and sheet resistance will be discussed later in detail.

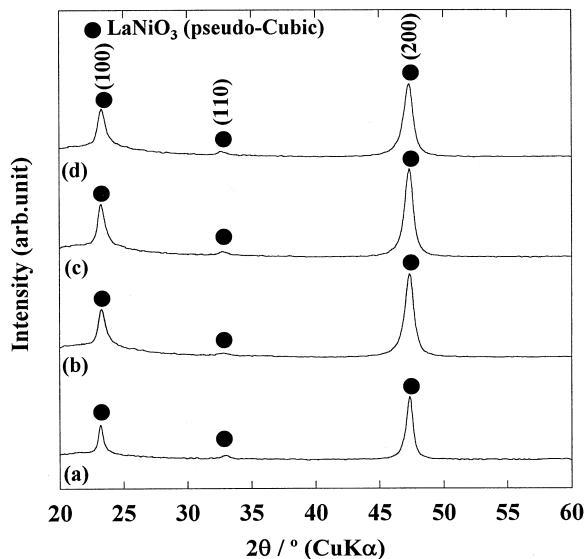


Fig. 2.  $\theta$ - $2\theta$  XRD profiles of  $\text{LaNiO}_3$  thin films on  $\text{SiO}_2$  glass substrates heated at  $700^\circ\text{C}$  for (a) 1 min, (b) 5 min, (c) 10 min and (d) 20 min and annealed at  $700^\circ\text{C}$  for 5 h in a flowing oxygen by process 2.

Table 1  
The orientation factor, the crystallite size and the sheet resistance of the LNO films on  $\text{SiO}_2$  glass substrate made by process 2

Heating time (min)	Annealing time (h)	Orientation factor $F$	Crystallite size (nm)	Sheet resistance $\rho_s (\Omega/\square)$
1	—	0.65	6.9	1680
1	5	0.91	17.5	53.5
1	10	0.95	19.5	55.6
5	—	0.86	9.2	256.6
5	5	0.92	13.4	114
5	10	0.94	14.1	101
10	—	0.90	12.1	136.4
10	5	0.92	13.0	88.6
10	10	0.95	13.0	80.1
20	—	0.90	10.9	126.6
20	5	0.90	13.4	128.0
20	10	0.95	13.6	106.1

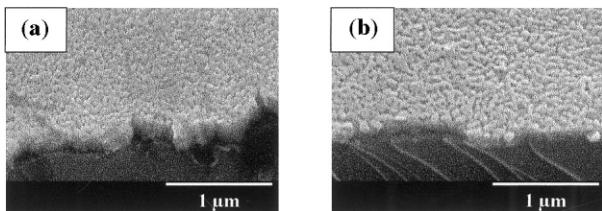


Fig. 3. FESEM photographs of  $\text{LaNiO}_3$  thin films on  $\text{SiO}_2$  made by (a) process 1 and (b) process 2 with heating for 10 min and annealing 1 h in a flowing oxygen.

Fig. 3 shows FESEM photographs of the LNO/ $\text{SiO}_2$  made by process (a) 1 and (b) process 2 with heating for 10 min and annealing for 1 h at  $700^\circ\text{C}$  in a flowing oxygen. The surface of the film made by process 2 is more porous than that made by process 1. However, the sheet resistance of the LNO film made by process 2 was lower than that by process 1. Thicknesses of the films made by processes 1 and 2 were 200 and 160 nm, respectively. The thickness of the other films made by each process was almost the same, regardless of the heating and annealing conditions.

The  $\text{CeO}_2$  thin films fabricated at various temperatures exhibited a high degree of orientation to the  $<100>$  direction (Table 2). LNO thin films were fabricated on the  $\text{CeO}_2$  films by heating at  $700^\circ\text{C}$  for 1 min by process 2 and annealing at  $700^\circ\text{C}$  for 5 h in a flowing oxygen. The  $F$  values of  $\text{CeO}_2$  films, the crystallite size and the sheet resistance of LNO/ $\text{CeO}_2$  films are shown in Table 2. Fig. 4 shows the  $\theta$ - $2\theta$  scan profiles of the LNO/ $\text{CeO}_2$ /Si structures. Strong (100) and (200) peaks of LNO are observed despite the different  $F$  values of  $\text{CeO}_2$  films. The sheet resistance of LNO were (a) 28.8, (b) 28.8, (c) 34.3 and (d)  $37.0 \Omega/\square$  for the sample shown in Fig. 4 (a), (b), (c) and (d), respectively. These values were as low as that of LNO/STO made by process 1. However, the resistivity was  $460 \mu\Omega\cdot\text{cm}$  and thickness was about 180 nm for the sample (a).

#### 4. Discussion

First, we discuss the difference in the degree of orientation of LNO/ $\text{SiO}_2$  films made by processes 1 and 2. In

Table 2  
The crystallite size and the sheet resistance of the LNO films on  $\text{CeO}_2$ /Si substrates

Fabrication temperature of $\text{CeO}_2$ on (100) Si substrate	Orientation factor of the $\text{CeO}_2$ films	Crystallite size of the LNO film (nm)	Sheet resistance $\rho_s$ of the LNO film ( $\Omega/\square$ )
400°C	0.62	23.8	28.8
500°C	0.58	22.6	28.8
600°C	0.87	22.2	34.3
700°C	0.82	24.7	37.0

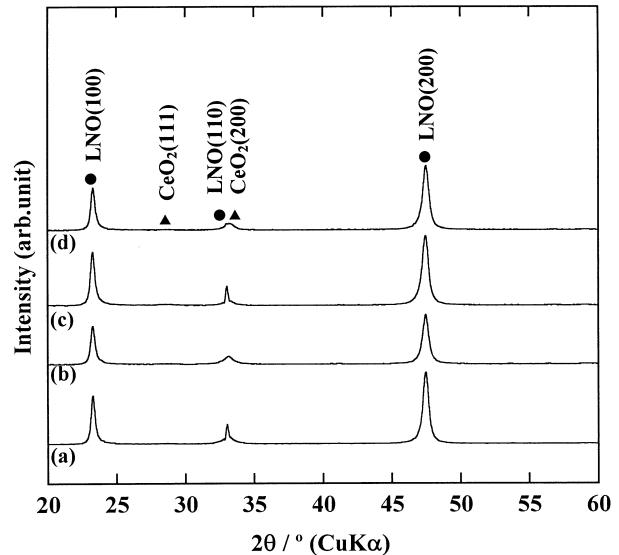


Fig. 4.  $\theta$ - $2\theta$  XRD profiles of  $\text{LaNiO}_3$  thin films heated at  $700^\circ\text{C}$  and annealed at  $700^\circ\text{C}$  for 5 h in a flowing oxygen by process 2 on  $\text{CeO}_2$ -covered Si substrates fabricated at (a)  $400^\circ\text{C}$ , (b)  $500^\circ\text{C}$ , (c)  $600^\circ\text{C}$  and (d)  $700^\circ\text{C}$ .

the case of process 2, most of LNO would nucleate heterogeneously from the substrate side. The (100)-plane of LNO which has the smallest surface energy could develop parallel to the substrate surface because grains in the film grow flat and outer surface is composed of the plane with the smallest surface energy, when adhesive bonding between the film and substrate is strong.<sup>12,13</sup> Therefore, the (100)-oriented LNO films could be fabricated even on the amorphous substrate. Grains in the film made by process 1 would nucleate homogeneously, resulting in the small degree of (100)-orientation.

Secondly, we discuss the effect of heating time during the deposition procedure on the sheet resistance. Fig. 5

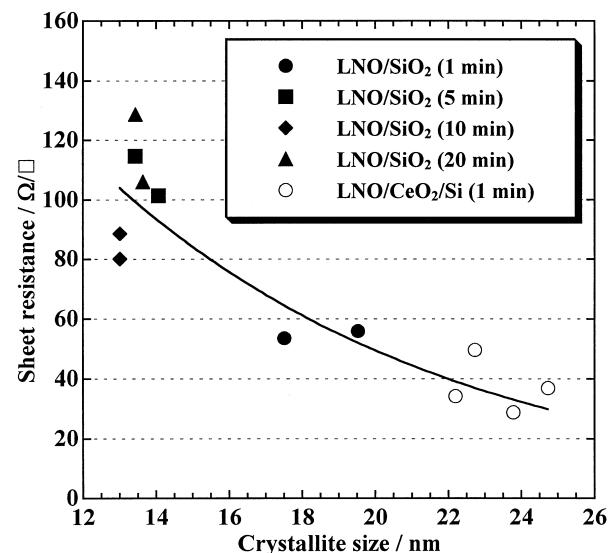


Fig. 5. Effect of crystallite size of  $\text{LaNiO}_3$  thin films on sheet resistance.

shows the relationship between the sheet resistance and the crystallite size of the LNO films. It is clearly shown that the sheet resistance decreases with increasing crystallite size of LNO. For the LNO/SiO<sub>2</sub> film, the crystallite size of LNO after annealing tends to increase with decreasing heating time during the deposition procedure. Before annealing the crystallite size of LNO/SiO<sub>2</sub> with short heating time (1 min) was smaller than that with longer heating time (5, 10 and 20 min), but that with short heating time was bigger than that with long heating time after annealing (Table 1). This is because small grains have large surface energy which acts as a driving force for grain growth of the LNO during annealing.

## 5. Conclusions

Highly (100)-oriented LaNiO<sub>3</sub> thin films were fabricated on (100)SrTiO<sub>3</sub>, (100)Si and SiO<sub>2</sub> glass substrates by the sol-gel method. Among them, the LNO/STO showed the lowest resistivity of 340  $\mu\Omega\cdot\text{cm}$ . (100)-Oriented LNO/CeO<sub>2</sub>/Si MIS structure with the sheet resistance of 28.8  $\Omega/\square$  could also be obtained. It was revealed that the electrical property of the films mainly depended on the crystallite size of LNO.

## References

- Lee, H. Y. and Wu, T. B., Crystallization kinetics of sputter-deposited LaNiO<sub>3</sub> thin films on Si substrate. *J. Mater. Res.*, 1998, **13**, 2291–2296.
- Wu, Di., Li, A., Liu, Z., Ling, H., Ge, C. Z., Liu, X., Wang, H., Wang, M., Lü, P. and Ming, N., Fabrication and electrical property of sol-gel derived (BaSr)TiO<sub>3</sub> thin films with metallic LaNiO<sub>3</sub> electrode. *Thin Solid Films*, 1998, **336**, 172–175.
- Rajeev, K. P., Shivashankar, G. V. and Raychaudhuri, A. K., Low-temperature electronic properties of a normal conducting perovskite oxide (LaNiO<sub>3</sub>). *Solid State Commun.*, 1991, **79**, 591–595.
- Kim, S. S., Kim, B. I., Park, Y. B. and Je, J. H., LaNiO<sub>3</sub> under-electrode layers for the growth of textured (Pb<sub>0.4</sub>Zr<sub>0.6</sub>)TiO<sub>3</sub> thin films using pulsed laser deposition. *Appl. Phys. A*, 1999, **69**, s625–s628.
- Hu, G. D., Wilson, I. H., Xu, J. B., Li, C. P. and Wong, S. P., Low-temperature preparation and characterization of SrBi<sub>2</sub>Ta<sub>2</sub>O<sub>9</sub> thin films on (100)-oriented LaNiO<sub>3</sub> electrodes. *Appl. Phys. Lett.*, 2000, **76**, 758–1760.
- Wong, K. H. and Choy, C. L., Low-temperature growth of epitaxial LaNiO<sub>3</sub>/Pb(Zr<sub>0.52</sub>Ti<sub>0.48</sub>)O<sub>3</sub>/LaNiO<sub>3</sub> on Si(100) by pulsed laser deposition. *J. Vac. Sci. Technol. A*, 2000, **18**, 79–82.
- Shyu, M. J., Hong, T. J., Yang, T. J. and Wu, T. B., Highly (100)-oriented thin films of sol-gel derived Pb[(Mg<sub>1/3</sub>Nb<sub>2/3</sub>)<sub>0.675</sub>Ti<sub>0.325</sub>]O<sub>3</sub> prepared on textured LaNiO<sub>3</sub> electrode. *Jpn. J. Appl. Phys.*, 1995, **34**, 3647–3653.
- Chen, M. S., Wu, J. M. and Wu, T. B., Effect of (100)-textured LaNiO<sub>3</sub> electrode on crystallization and properties of sol-gel-derived Pb(Zr<sub>0.53</sub>Ti<sub>0.47</sub>)O<sub>3</sub> thin films. *Jpn. J. Appl. Phys.*, 1995, **34**, 4870–4875.
- Shy, H. J. and Wu, T. B., Effect of bottom electrode on the structural and characteristics of barium titanate thin films. *Jpn. J. Appl. Phys.*, 1998, **37**, 4049–4055.
- Shy, H. J. and Wu, T. B., Structural and electrical characteristics of Ba(Zr<sub>0.12</sub>Ti<sub>0.88</sub>)O<sub>3</sub> thin films deposited on LaNiO<sub>3</sub> electrode by rf magnetron sputtering. *Jpn. J. Appl. Phys.*, 1998, **37**, 5638–5644.
- Ami, T. and Suzuki, M., MOCVD growth of (100)-oriented CeO<sub>2</sub> thin films on hydrogen-terminated Si (100) substrates. *Mater. Sci. Eng.*, 1998, **B54**, 84–91.
- Mashita, M. and Yoshida, M., Handbook of thin film engineering. *Kodansha*, 1998, pp.188 (in Japanese).
- Kern, R., Lay, G. L. and Metois, J. J., Basic mechanisms in the early stages of epitaxy. *Current Topics in Materials Science*, 1979, **3**, 130.